



ESIPT-based fluorescence probe for the rapid detection of hypochlorite (HOCl/CIO⁻)[†]

Luling Wu,^a Qingye Yang,^b Liyuan Liu,^a Adam C. Sedgwick,^a Alexander J. Cresswell,^a Steven D. Bull,^a Chusen Huang^b and Tony D. James^{a,c}

Cite this: *Chem. Commun.*, 2018, 54, 8522

Received 8th May 2018,
Accepted 28th June 2018

DOI: 10.1039/c8cc03717e

rsc.li/chemcomm

ESIPT-based fluorescence probes are emerging as an attractive tool for the detection of biologically relevant analytes owing to their unique photophysical properties. In this work, we have developed an ESIPT-based fluorescence probe (TCBT-OMe) for the detection of HOCl/CIO⁻ through the attachment of a bioorthogonal dimethylthiocarbamate linker. TCBT-OMe was shown to rapidly detect HOCl/CIO⁻ (<10 s) at biologically relevant concentrations (LoD = 0.16 nM) and have an excellent selectivity towards others ROS/RNS and amino acids. Therefore, TCBT-OMe was tested in live cells and was successfully shown to be able to detect endogenous and exogenous HOCl/CIO⁻ in HeLa cells. Additionally, TCBT-OMe acts as a dual input logic gate for Hg²⁺ and H₂O₂. Interestingly, Hg²⁺ alone gradually causes a fluorescence response but requires >30 min to produce a fluorescence response. Test strips containing TCBT-OMe were prepared and were demonstrated as an effective way to detect HOCl/CIO⁻ in water. Furthermore, TCBT-OMe was shown to detect exogenously added HOCl/CIO⁻ in three different water samples with little interference thus demonstrating the effectiveness as a method for the detection of HOCl/CIO⁻ in drinking water samples.

Hypochlorous acid (HOCl) is a biologically important reactive oxygen species (ROS), which partially dissociates to form its hypochlorite anion (CIO⁻) under physiological conditions. In biological systems, myeloperoxidase, an enzyme found in leukocytes produces HOCl/CIO⁻ by catalysing the reaction between Cl + H₂O₂ → HOCl.¹ This vital ROS is used in immune defence systems due to its microbicidal properties.¹ Unfortunately, excessive

production of HOCl/CIO⁻ can lead to the damage of a range of biological targets such as amino acids, proteins, carbohydrates and lipids.^{2,3} As a consequence, HOCl/CIO⁻ has been associated with a number of diseases causing cell and tissue damage.⁴

In addition to its role in biological systems, HOCl/CIO⁻ is produced by the chlorination of water (Cl₂ + H₂O → HOCl), which is the most common method for the treatment of water especially in public swimming pools.⁵ NaOCl (Bleach) is also extensively used as a disinfectant for both domestic and industrial purposes. Unfortunately, over-exposure to HOCl/CIO⁻, results in swimming pool-associated asthma, irritation to the oesophagus, throat and spontaneous vomiting (http://www.who.int/water_sanitation_health/dwq/chlorine.pdf).⁶ Additionally, there is an increased risk of bladder cancer associated with chlorinated by-products produced from chlorinated water.^{7,8} Therefore, given the potential health hazard towards animals and humans, the development of an effective method for HOCl/CIO⁻ detection is required.

Within our research group, we are interested in developing reaction-based fluorescence sensors for the detection of biologically important analytes.^{9–13} Small-molecule fluorescence probes are a particular attractive tool owing to their high sensitivity, selectivity and high spatial and temporal resolution.¹⁴ In particular, we are interested in using Excited State Intramolecular Proton Transfer (ESIPT)-based fluorescence probes due to their excellent photophysical properties, which include intense luminescence, photostability and a large Stokes shift.^{15,16} Previously, we reported an ESIPT-based fluorescence probe for the detection of peroxyxynitrite (ONOO⁻) through the use of a benzyl boronic ester protecting group (Scheme 1).¹⁵ This protecting group blocked the ESIPT process and therefore a low fluorescence intensity was observed. The addition of ONOO⁻, resulted in the fluorophore's deprotection and an increase in fluorescence intensity was observed.

In this work, we believed a methoxy-hydroxybenzothiazole (HBT-OMe) fluorophore would provide an effective ESIPT fluorescence probe for the detection of HOCl/CIO⁻ (see ESI,† S1).^{17,18}

To obtain TCBT-OMe we first prepared HBT-OMe by the addition of a 2 : 1 H₂O₂–(30% in H₂O)/HCl solution to 2-aminothiophenol

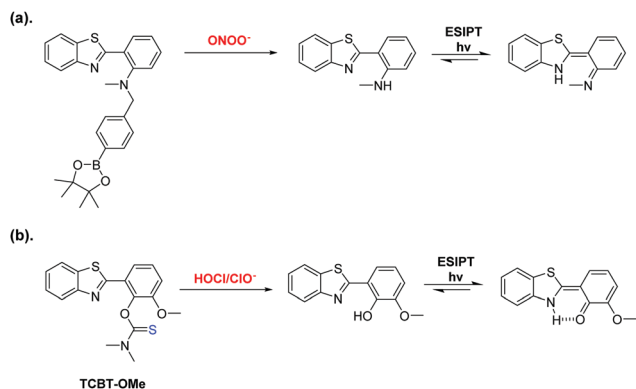
^a Department of Chemistry, University of Bath, Bath, BA2 7AY, UK.
E-mail: t.d.james@bath.ac.uk, s.d.bull@bath.ac.uk, a.c.sedgwick@bath.ac.uk, a.j.cresswell@bath.ac.uk

^b The Education Ministry Key Laboratory of Resource Chemistry, Shanghai Key Laboratory of Rare Earth Functional Materials, and Shanghai Municipal Education Committee Key Laboratory of Molecular Imaging Probes and Sensors, Department of Chemistry, Shanghai Normal University, 100 Guilin Road, Shanghai 200234, China. E-mail: huangcs@shnu.edu.cn

^c Department of Materials and Life Sciences, Faculty of Science and Technology, Sophia University, 7-1 Kioi-cho, Chiyoda-ku, Tokyo 102-8554, Japan

† Electronic supplementary information (ESI) available. See DOI: 10.1039/c8cc03717e





Scheme 1 (a) Our previously reported ESPIPT probe for the detection of ONOO^- . (b) This work – a thiocarbamate linker-based ESPIPT **TCBT-OMe** for the detection of HOCl/CIO^- .

and *O*-vanillin in EtOH. This reaction proceeded quickly and smoothly, in a good yield (68%). With **HBT-OMe** in hand, four equivalents of dimethylthiocarbamoyl chloride was then added slowly to a solution of **HBT-OMe** in DCM. DIPEA was subsequently added dropwise to the reaction, which produced **TCBT-OMe** in excellent yield (72%).

We then evaluated the UV-Vis of **TCBT-OMe** with the addition of HOCl/CIO^- (10 μM), which resulted in the formation of a UV absorption peak at ~ 310 nm (see ESI,† Fig. S1). Bhattacharyya *et al.* have reported that the fluorescence emission of the ESPIPT process can be effected by intermolecular hydrogen bonding.^{19,20} Therefore, evaluation of ESPIPT-based fluorescence probes are commonly carried out in the presence of the surfactant cetyl trimethylammonium bromide (CTAB, 1 mM) or by using a large ratio of organic solvent.^{19,21–23} It is believed that the formation of a micellar environment creates a hydrophobic pocket that aids the ESPIPT process. Therefore, we evaluated the ability of **TCBT-OMe** to detect HOCl/CIO^- by fluorescence in the presence of CTAB, 1 mM. As shown in Fig. 1a, **TCBT-OMe** was found to be very sensitive towards HOCl/CIO^- reacting with micromolar concentrations to produce a large increase in fluorescence (~ 42 fold – Fig. S3, ESI†). **TCBT-OMe** was shown to rapidly react with HOCl/CIO^- producing a fluorescence response within less than 10 s (see ESI,† Fig. S4) and have a very low Limit of Detection (LoD) of 0.16 nM (see ESI,† Fig. S5). HOCl/CIO^- (35 μM) was added to **TCBT-OMe** at different pH values and a bell-shaped curve was observed. The largest fluorescence response was seen at the $\text{p}K_a$ of $\text{HOCl/CIO}^- = 7.53$ (Fig. S5, ESI†) suggestive of general acid–base catalysis being in operation. (see ESI,† Scheme S1 for proposed mechanism).

We then evaluated the selectivity of **TCBT-OMe** towards other reactive oxygen/nitrogen species (ROS/RNS) and amino acids (Fig. 1b). Remarkably, **TCBT-OMe** had an excellent selectivity towards HOCl/CIO^- therefore permitting its use as a fluorescence probe for the detection of HOCl/CIO^- in live cells. As shown in Fig. 2, **TCBT-OMe** was successfully used to visualise endogenously stimulated HOCl/CIO^- in HeLa cells using phorbol 12-myristate 13-acetate (**PMA**, which is a ROS stimulant that induces the production of HOCl/CIO^-). Separately, HeLa cells were



Fig. 1 (a) Fluorescence spectra of **TCBT-OMe** (5 μM) with increasing additions of HOCl/CIO^- (from 0 to 17 μM) in PBS buffer (pH 7.4, containing 1% DMSO, 1 mM CTAB). Measurements were taken after 1 min. $\lambda_{\text{ex}} = 310$ nm. Slit widths: ex = 6 nm em = 4 nm. (b) Selectivity bar chart of **TCBT-OMe** in PBS pH 7.4, containing 1% DMSO, 1 mM CTAB with HClO (15 μM) and other interfering reagents (ROS/RNS and various amino acids). 1, HClO ; 2, blank; 3, ONOO^- ; 4, H_2O_2 ; 5, ROO^* ; 6, $\bullet\text{OH}$; 7, $\bullet\text{O}_2^-$; 8, $^1\text{O}_2$; 9, NO; 10, glycine; 11, asparagine; 12, cysteine; 13, homocysteine; 14, glutathione; 15, arginine; 16, histidine; 17, serine; 18, glycine; 19, threonine. Note: the concentration of **TCBT-OMe** and each interfering species are 5 μM and 100 μM respectively, 30 min wait before measurement in buffer solution. $\lambda_{\text{ex}} = 310$ nm/ $\lambda_{\text{em}} = 472$ nm error bars represent s.d. Measurements were taken after 30 min. $\lambda_{\text{ex}} = 310$ nm. Slit widths: ex = 6 nm, em = 4 nm.

also pretreated with 4-aminobenzoic acid hydrazide (**ABAH**, which is a specific inhibitor of MPO which suppressed the generation of HOCl) and as expected only weak fluorescence was observed. **TCBT-OMe** was also able to detect HOCl/CIO^- added exogenously to the HeLa cells.

The dimethylthiocarbamate linker of **TCBT-OMe** has previously been used in the construction of dual input molecular logic gate²⁴ for the detection of Hg^{2+} 'AND' H_2O_2 (see ESI† Scheme S2 for proposed mechanism).^{25,26} Therefore, we evaluated the ability of **TCBT-OMe** to perform molecular logic with the input of Hg^{2+} and H_2O_2 . The presence of solely H_2O_2 (120 μM) led to a small increase in fluorescence intensity (dashed line), however, with subsequent additions of Hg^{2+} (0–9 μM) a large fluorescence response was observed (Fig. 3a). To demonstrate that both analytes are required, Hg^{2+} was added first, followed by the addition of H_2O_2 (0–180 μM). As shown in Fig. 3b, the subsequent addition of H_2O_2 rapidly led to an increase in fluorescence intensity. **TCBT-OMe** was shown to be selective towards Hg^{2+} over other metal cations in the presence of H_2O_2 (see ESI,† Fig. S9). Interestingly, Hg^{2+} alone resulted in a slow increase in fluorescence intensity (see ESI,† Fig. S10). This is believed to be



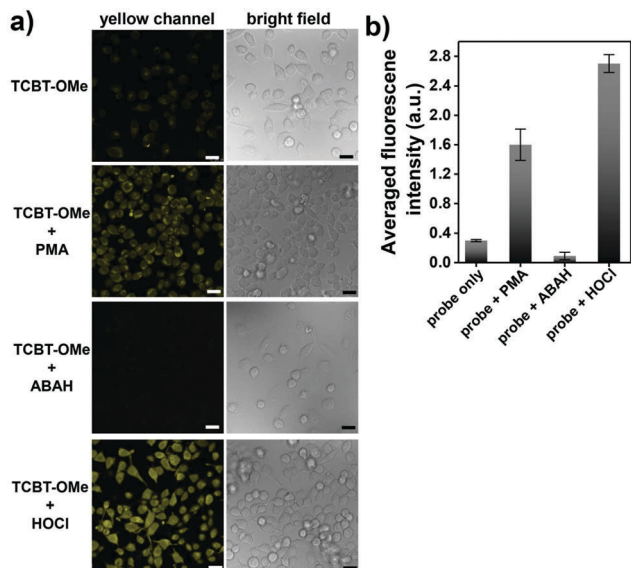


Fig. 2 (a) From top to bottom: HeLa cells were pretreated with **TCBT-OMe** (40 μM) for 30 min; HeLa cells pretreated with **TCBT-OMe** (40 μM) were then left for 30 min after preincubation with PMA (1.2 $\mu\text{g mL}^{-1}$) for 90 min; HeLa cells pretreated with **TCBT-OMe** (40 μM) were then left for 30 min after preincubation with 250 μM ABAH for 70 min; HeLa cells loaded with **TCBT-OMe** (40 μM) for 30 min followed by the exogenous addition of 8 μM NaOCl for 5 min. Scale bar: 25 μm $\lambda_{\text{ex}} = 420 \text{ nm}$ / $\lambda_{\text{em}} = 420\text{--}590 \text{ nm}$. (b) The histogram shows the semi-quantitative calculation of averaged fluorescence intensity (FI) of each fluorescence panel in the displayed images by ImageJ software.

due to the instability of the dimethylcarbonate formed from the reaction of **TCBT-OMe** with Hg^{2+} .

Despite this interesting dual responsive reactivity of **TCBT-OMe**, this 'AND' logic requires minutes to fully react, whereas HOCl/ClO^- reacts with **TCBT-OMe** within seconds. Therefore, due to the significantly greater reactivity of **TCBT-OMe** towards HOCl/ClO^- over Hg^{2+} , we believed we could use it as an effective method for the detection of HOCl/ClO^- in drinking water sources.

We produced test strips by simply soaking a commercially available test strip in water containing **TCBT-OMe** (0.8 mM). After drying, test strips impregnated with **TCBT-OMe** were placed in water containing HClO/ClO^- (0–200 μM). As shown in Fig. 4, there is a clear colour/intensity difference in the test strips that have been dipped into water containing various concentrations of HClO/ClO^- .

In addition to detecting HClO/ClO^- in water, **TCBT-OMe** was added into three different water samples containing 1 mM CTAB (Sample A, tap water from University of Bath; Sample B, water from the Avon River (Bath); Sample C, water from Roman spa in Bath). Interestingly, little interference was observed for the exogenous addition of HClO/ClO^- to each water sample (>95% recovery) – see ESI,† Table S1.

In summary, we have developed an ESIPT-based fluorescence **TCBT-OMe** for the detection of HClO/ClO^- . **TCBT-OMe** was shown to have a very high sensitivity and selectivity towards HClO/ClO^- fully reacting within 10 s and having a LoD of 0.16 μM . Significantly, **TCBT-OMe** was able to detect endogenous and

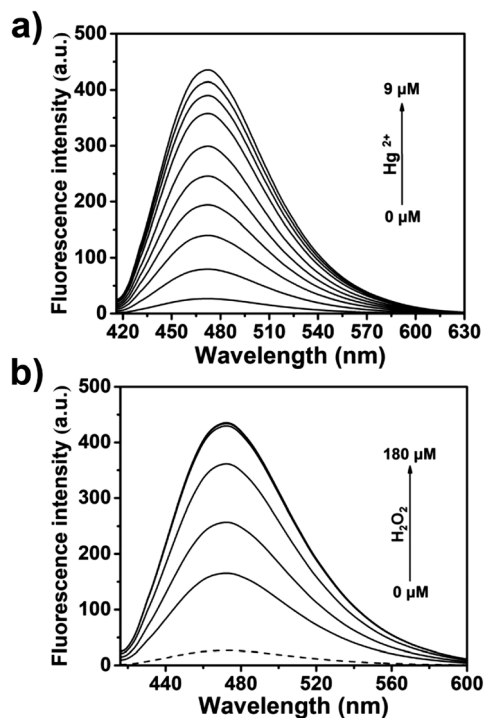


Fig. 3 (a) Fluorescence spectra of **TCBT-OMe** (5 μM) in the presence of H_2O_2 (120 μM) – (dashed line represent probe and H_2O_2) with increasing concentrations of Hg^{2+} (0–9 μM) in buffer solution pH 7.4, 1% DMSO, 1 mM CTAB 14 min wait between measurement. $\lambda = 310 \text{ nm}$. Slit widths: $\text{ex} = 6 \text{ nm}$ $\text{em} = 4 \text{ nm}$. (b) Fluorescence spectra of **TCBT-OMe** (5 μM) in the presence of Hg^{2+} (9 μM) – (dashed line represents probe and Hg^{2+}) with increasing concentrations of H_2O_2 (final concentration: 0, 20, 40, 80, 100, 120, 140 μM and 180 μM) in PBS pH 7.4, containing 1% DMSO, 1 mM CTAB. 14 min wait between measurement in buffer solution. $\lambda_{\text{ex}} = 310 \text{ nm}$. Slit widths: $\text{ex} = 6 \text{ nm}$ $\text{em} = 4 \text{ nm}$.

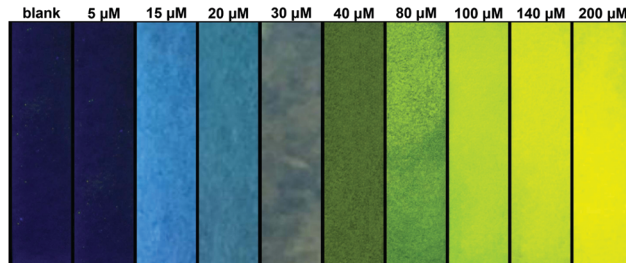


Fig. 4 Photograph showing the colour changes of **TCBT-OMe** impregnated test strips after addition to water samples containing different concentrations of HClO/ClO^- under UV light (365 nm).

exogenous HClO/ClO^- in HeLa cells. Additionally, **TCBT-OMe** was shown as a dual input logic gate with Hg^{2+} and H_2O_2 as inputs. Interestingly, Hg^{2+} alone gradually produced a fluorescence response but required >30 min to produce a significant fluorescence response. Test strips containing **TCBT-OMe** were developed and shown to be an effective way to detect HClO/ClO^- in water. Furthermore, **TCBT-OMe** was shown to detect exogenously added HClO/ClO^- in three different water samples with little interference demonstrating its effectiveness as a method to detect HClO/ClO^- in drinking water samples.



LW wishes to thank China Scholarship Council and the University of Bath for supporting his PhD work in the UK. We would like to thank the EPSRC and the University of Bath for funding. ACS thanks the EPSRC for a studentship. AJC wishes to thank the Royal Society for a University Research Fellowship. TDJ wishes to thank the Royal Society for a Wolfson Research Merit Award and Sophia University for a visiting professorship. NMR characterisation facilities were provided through the Chemical Characterisation and Analysis Facility (CCAF) at the University of Bath (www.bath.ac.uk/ccaf). The EPSRC UK National Mass Spectrometry Facility at Swansea University is thanked for analyses. All data supporting this study are provided as supplementary information accompanying this paper (ESI†).

Conflicts of interest

No conflicts of interest.

Notes and references

- 1 A. Strzepa, K. A. Pritchard and B. N. Dittel, *Cell. Immunol.*, 2017, **317**, 1–8.
- 2 M. J. Davies, *J. Clin. Biochem. Nutr.*, 2011, **48**, 8–19.
- 3 S. J. Klebanoff, *J. Leukocyte Biol.*, 2005, **77**, 598–625.
- 4 B. S. van der Veen, M. P. J. de Winther and P. Heeringa, *Antioxid. Redox Signaling*, 2009, **11**, 2899–2937.
- 5 L. Kunigk, R. Gedraite and C. J. Kunigk, *Environ. Eng. Manage. J.*, 2018, **17**, 711–720.
- 6 C. Zwiener, S. D. Richardson, D. M. De Marini, T. Grummt, T. Glauner and F. H. Frimmel, *Environ. Sci. Technol.*, 2007, **41**, 363–372.
- 7 K. P. Cantor, R. Hoover, P. Hartge, T. J. Mason, D. T. Silverman, R. Altman, D. F. Austin, M. A. Child, C. R. Key, L. D. Marrett, M. H. Myers, A. S. Narayana, L. I. Levin, J. W. Sullivan, G. M. Swanson, D. B. Thomas and D. W. West, *J. Natl. Cancer Inst.*, 1987, **79**, 1269–1279.
- 8 C. M. Villanueva, K. P. Cantor, S. Cordier, J. J. K. Jaakkola, W. D. King, C. F. Lynch, S. Porru and M. Kogevinas, *Epidemiol.*, 2004, **15**, 357–367.
- 9 A. C. Sedgwick, R. S. L. Chapman, J. E. Gardiner, L. R. Peacock, G. Kim, J. Yoon, S. D. Bull and T. D. James, *Chem. Commun.*, 2017, **53**, 10441–10443.
- 10 C. M. Lopez-Alled, A. Sanchez-Fernandez, K. J. Edler, A. C. Sedgwick, S. D. Bull, C. L. McMullin, G. Kociok-Kohn, T. D. James, J. Wenk and S. E. Lewis, *Chem. Commun.*, 2017, **53**, 12580–12583.
- 11 A. C. Sedgwick, H. H. Han, J. E. Gardiner, S. D. Bull, X. P. He and T. D. James, *Chem. Commun.*, 2017, **53**, 12822–12825.
- 12 D. Wu, A. C. Sedgwick, T. Gunnlaugsson, E. U. Akkaya, J. Yoon and T. D. James, *Chem. Soc. Rev.*, 2017, **46**, 7105–7123.
- 13 E. V. Lampard, A. C. Sedgwick, X. L. Sun, K. L. Filer, S. C. Hewins, G. Kim, J. Yoon, S. D. Bull and T. D. James, *ChemistryOpen*, 2018, **7**, 262–265.
- 14 J. Chan, S. C. Dodani and C. J. Chang, *Nat. Chem.*, 2012, **4**, 973–984.
- 15 A. C. Sedgwick, X. L. Sun, G. Kim, J. Yoon, S. D. Bull and T. D. James, *Chem. Commun.*, 2016, **52**, 12350–12352.
- 16 J. S. Wu, W. M. Liu, J. C. Ge, H. Y. Zhang and P. F. Wang, *Chem. Soc. Rev.*, 2011, **40**, 3483–3495.
- 17 B. C. Zhu, P. Li, W. Shu, X. Wang, C. Y. Liu, Y. Wang, Z. K. Wang, Y. W. Wang and B. Tang, *Anal. Chem.*, 2016, **88**, 12532–12538.
- 18 B. C. Zhu, L. Wu, M. Zhang, Y. W. Wang, Z. Y. Zhao, Z. K. Wang, Q. X. Duan, P. Jia and C. Y. Liu, *Sens. Actuators, B*, 2018, **263**, 103–108.
- 19 N. Sarkar, K. Das, S. Das, A. Datta, D. Nath and K. Bhattacharyya, *J. Phys. Chem.*, 1995, **99**, 17711–17714.
- 20 K. Das, N. Sarkar, A. K. Ghosh, D. Majumdar, D. N. Nath and K. Bhattacharyya, *J. Phys. Chem.*, 1994, **98**, 9126–9132.
- 21 D. P. Murale, H. Kim, W. S. Choi and D. G. Churchill, *Org. Lett.*, 2013, **15**, 3946–3949.
- 22 H. R. Zheng, L. Y. Niu, Y. Z. Chen, L. Z. Wu, C. H. Tung and Q. Z. Yang, *Chin. Chem. Lett.*, 2016, **27**, 1793–1796.
- 23 R. Hu, J. A. Feng, D. H. Hu, S. Q. Wang, S. Y. Li, Y. Li and G. Q. Yang, *Angew. Chem., Int. Ed.*, 2010, **49**, 4915–4918.
- 24 S. Erbas-Cakmak, S. Kolemen, A. C. Sedgwick, T. Gunnlaugsson, T. D. James, J. Yoon and E. U. Akkaya, *Chem. Soc. Rev.*, 2018, **47**, 2228–2248.
- 25 D. P. Murale, H. Liew, Y. H. Suh and D. G. Churchill, *Anal. Methods*, 2013, **5**, 2650–2652.
- 26 W. Shu, L. G. Yan, J. Liu, Z. K. Wang, S. Zhang, C. C. Tang, C. Y. Liu, B. C. Zhu and B. Du, *Ind. Eng. Chem. Res.*, 2015, **54**, 8056–8062.

